
PHYSICAL-CHEMICAL PROCESSES OF CLOUD ACTIVATION STUDIED WITH A DESKTOP CLOUD MODEL

Stephen E. Schwartz

ses@bnl.gov

Brookhaven National Laboratory
Upton NY USA 11973

6th International Conference
Air-Surface Exchange of Gases and Particles
Edinburgh, Scotland U.K.
July 3-7, 2000

Abstract

A model of the activation process of a zero-dimensional cloud is described. The model runs in *Mathematica*®, a platform-independent environment for numerical computation. Key input parameters are updraft velocity and the dry distribution of number and composition of aerosol particles; 25 bins in the dry radius range 9 to 280 nm provide an accurate representation of microphysical dynamics. As the parcel is cooled water vapor is taken up by aerosol particles, governed by the difference between the ambient water vapor partial pressure and the equilibrium partial pressure above each drop, as given by the Köhler expression. As environmental supersaturation increases, initially larger particles, and then successively smaller particles may activate. The environmental supersaturation reaches a maximum and then decreases, effectively limiting the radius range of activated particles. This "desktop cloud" can be used to explore a variety of phenomena: the dependence of maximum supersaturation on environmental variables such as updraft velocity, aerosol properties and the presence of soluble and/or reactive gases; to examine the locus of uptake and aqueous-phase reaction of gases and the resultant influence on the particle size distribution; and to test parametrizations of aerosol influences on cloud microphysics.

PHYSICAL-CHEMICAL PROCESSES OF CLOUD ACTIVATION STUDIED WITH A DESKTOP CLOUD MODEL

Stephen E. Schwartz

ses@bnl.gov

Brookhaven National
Laboratory



Work in Progress



Background

Clouds form when air containing water vapor and aerosol particles is cooled below the dew point. Water vapor condenses on aerosol particles.

The equilibrium vapor pressure of water $p(a)$ above a liquid water drop of radius a is controlled by **Raoult's law** (vapor pressure lowering by solute) and the **Kelvin equation** (free energy of surface tension) and is strongly a function of drop radius, according to the **Köhler expression** (1923, 1936):

$$p(a) = p_w(T) \exp \left[\underbrace{\frac{2M_w\sigma}{R_g T \rho a}}_{\text{Kelvin}} - \underbrace{\frac{\nu m_s / M_s}{(\frac{4}{3}\pi a^3 \rho - m_s) / M_w}}_{\text{Raoult}} \right]$$

where $p_w(T)$ is the saturation vapor pressure of pure water at the ambient temperature

M_w, M_s are the molecular weights of water and solute

σ is the solution - air surface tension

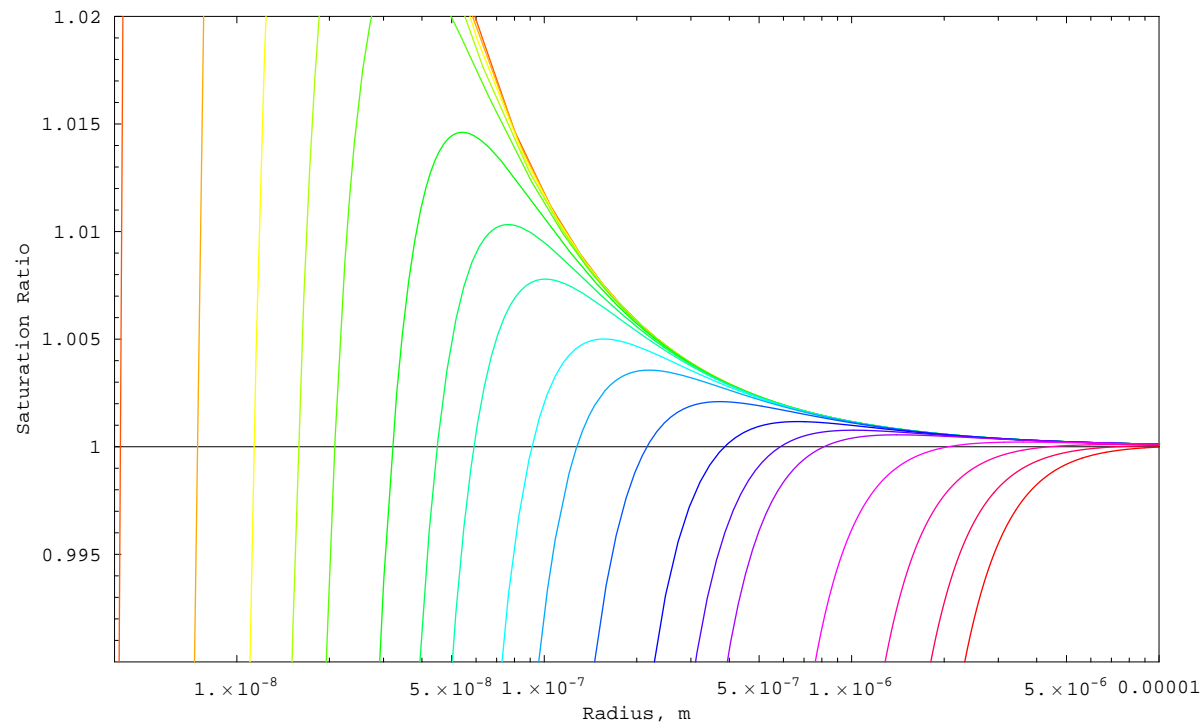
R_g is the gas constant; T is the temperature

ρ is the solution density

ν is the van't Hoff factor (equiv / mol) including nonideality corrections

m_s is the solute mass

Köhler curves give saturation ratio vs. radius for fixed solute mass per particle:



Critical saturation is maximum in curve; **critical radius** is corresponding radius value. Critical saturation decreases with increasing solute mass.

Cloud Droplet Activation

Activation of an aerosol particle to form a cloud droplet occurs when the environmental water vapor pressure exceeds Köhler maximum, with resultant condensation of water vapor, sufficiently long for the drop radius to exceed the corresponding critical radius.

- Once activated the drop grows under kinetic control.
- Activation is inherently **kinetic**, being controlled mainly by vapor-phase diffusion and heat transfer.

During cloud formation the environmental supersaturation in a given air parcel typically exhibits a **short transient maximum** triggered by initial adiabatic cooling and quenched by condensation of water vapor onto the newly available surface area of the activated cloud droplets, which serves as a runaway sink for water vapor.

The time history of the saturation ratio depends intrinsically on the interaction of water vapor with aerosol and gaseous solutes.

Importance

Cloud droplet activation determines the droplet number concentration and size distribution of the resultant cloud and the distribution of soluble gases taken up in the cloudwater.

The efficiency of activation of aerosol particles is of interest in cloud chemistry and microphysics.

- Major influence on **deposition** of aerosol materials in rain.
- An enhanced concentration of cloud droplets can **suppress precipitation**.
- The radiative properties of clouds: A greater concentration of aerosol particles generally results in a greater concentration of cloud droplets and **brighter clouds**.

These phenomena are important in considerations of **anthropogenic climate change**.

This Study. . .

Examines the dependence of cloud droplet activation on controlling processes by examining its **kinetics**.

Examines the time constants of droplet growth relative to duration of maximum supersaturation, gaseous diffusion, and the like.

Provides a differentiated picture of growth of size classes of drops and their uptake of water vapor and soluble gases.

Provides dependence of cloud droplet activation on controlling parameters that can be used to test approximations suitable for large scale atmospheric models.

Approach

Zero-Dimensional box model describing increase in water vapor saturation ratio and resultant mass-transfer processes pertinent to cloud formation.

Cloud updraft velocity and initial aerosol populations are treated as independent variables.

Updraft velocity is treated as constant in results reported here, but any time-dependent updraft velocity can be employed.

Temperature decrease due to updraft velocity is manifested in the difference between ambient partial pressure of water and equilibrium partial pressure as given by the Clausius-Clapeyron equation.

Coagulation and precipitation development are not represented in the model.

Soluble gases (e.g. HNO_3) can be added and their fate and influence as solute can be determined.

Kinetics of mass transport processes are examined by solution of coupled differential equations describing the radii of classes of aerosol particles using *Mathematica*®.

Key Independent Variables

- Number and size of aerosol particles
 - Updraft velocity
 - Presence or absence of soluble gas (HNO_3)
-

Thermodynamic Driving Force

Temperature change as a function of time $\Delta T(t)$ is given by **updraft velocity** w and **lapse rate** $g / c_{p,a}$, taking into account **latent heat release** due to condensed water:

$$\Delta T(t) = - \underbrace{\frac{gwt}{c_{p,a}}}_{\text{Lapse rate}} + \underbrace{\frac{C_w L_w}{\rho_a c_{p,a}}}_{\text{Latent heat}}$$

where g is the acceleration of gravity

$c_{p,a}$ is the heat capacity of air at constant pressure

C_w is liquid water content, kg m^{-3}

L_w is the latent heat of condensation of water vapor, J kg^{-1}

ρ_a is the density of air

Change in **equilibrium vapor pressure of water** (driving force for water condensation) is given by the Clausius-Calpeyron equation as

$$\Delta p_w(t) = \exp \left[- \frac{L_w M_w \Delta T(t)}{R_g T^2} \right]$$

Droplet Growth Equations

The **rate of accretion of water mass** is governed by molecular diffusion:

$$\frac{dm_{w,i}}{dt} = M_w(4\pi a_i^2) \cdot \frac{D_{\text{eff},w,i}}{a_i} \cdot [p_w(\infty) - p_w(a_i)] / R_g T$$

where M_w is the molecular weight of water

$m_{w,i}$ is the mass of water in a single drop of class i

a_i is the radius of drop of class i

$p_w(a_i)$, $p_w(\infty)$ are the gas - phase partial pressure of water at the drop surface and in the bulk, respectively, and

$D_{\text{eff},w,i}$ is the effective diffusion coefficient of water vapor for drop of class i

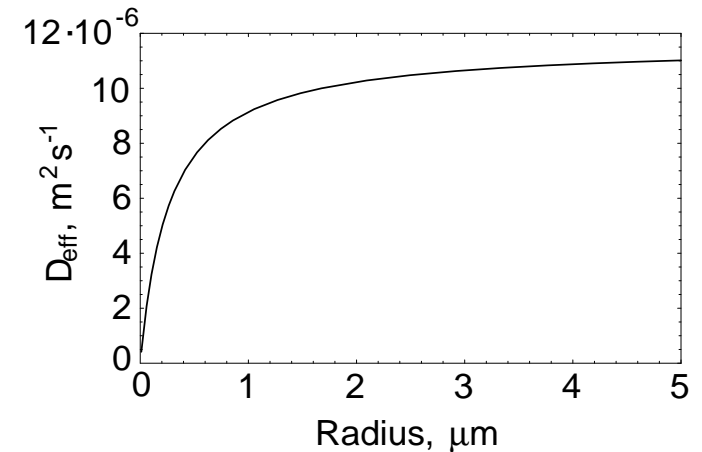
The corresponding **radial growth equation** is

$$\frac{da_i}{dt} = \frac{1}{(4\pi a_i^2)\rho} \frac{dm_{w,i}}{dt} = \frac{1}{a_i} \frac{M_w}{\rho} D_{\text{eff},w,i} \cdot [p_w(\infty) - p_w(a_i)] / R_g T$$

Radial growth rate is inversely proportional to the radius. Small drops “catch up” with large drops, narrowing the radius spectrum.

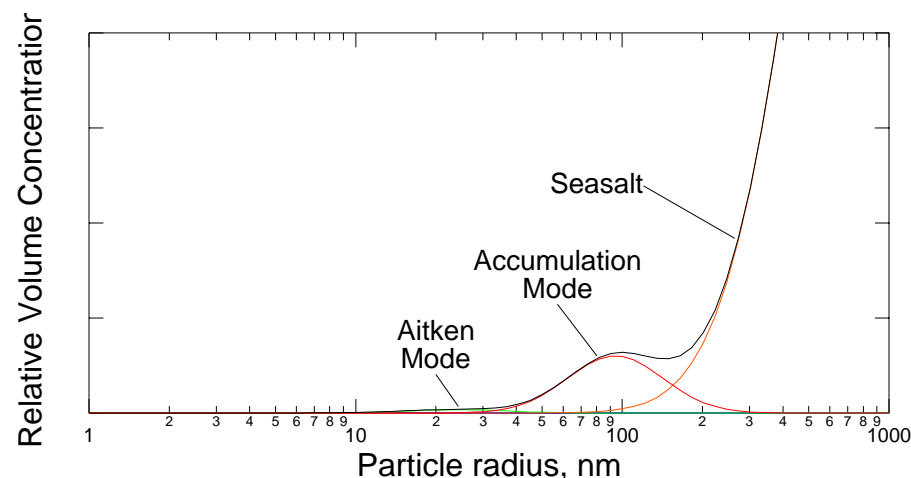
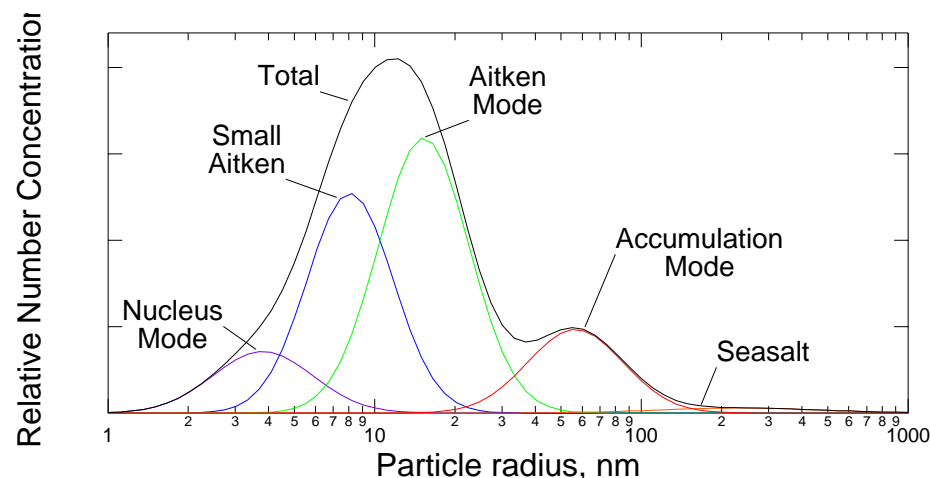
The **effective diffusion coefficient** $D_{\text{eff},w}$ of water vapor takes into account inhibition of mass transfer due to latent heat release on condensation and mass and thermal accommodation at the air-water interface:

$$D_{\text{eff},w} = \frac{1}{\underbrace{\frac{1}{D_w}}_{\text{Molecular Diffusion}} + \underbrace{\frac{1}{\frac{1}{4}\bar{v}_w a \alpha}}_{\text{Mass Accommodation}} + \underbrace{\frac{L_w^2 M_w^2 p_w(\infty)}{R_g^2 T^3}}_{\text{Latent Heat Release}} \left(\underbrace{\frac{1}{k_a}}_{\text{Thermal Conductivity}} + \underbrace{\frac{1}{\frac{1}{4}\bar{v}_a \rho_a c_{p,a} \beta}}_{\text{Thermal Accom.}} \right)}$$



where D_w is the diffusion coefficient of water vapor in air
 k_a is the thermal conductivity of air
 \bar{v}_w, \bar{v}_a are the mean molecular velocities of water vapor and air
 α, β are mass and thermal accommodation coefficients (0.5, 1)
 L_w is the latent heat of condensation of water vapor
 ρ_a is the density of air
 $c_{p,a}$ is the heat capacity of air at constant pressure

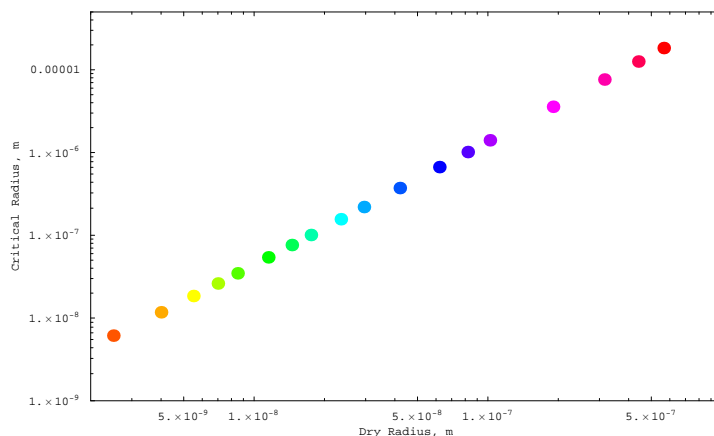
Size Distribution that served as Basis of Calculations



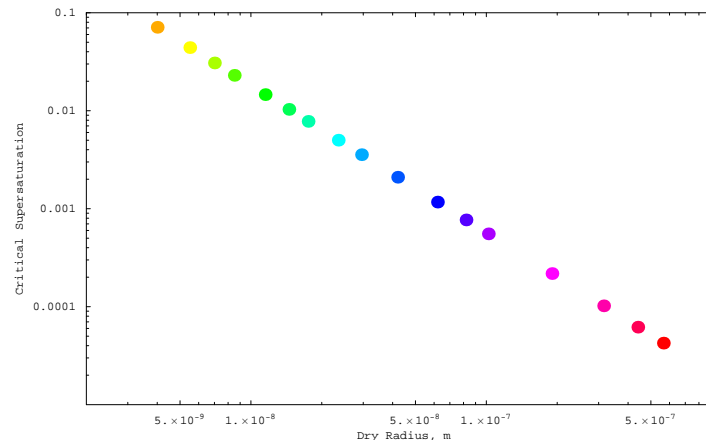
Seasalt, though low in number, dominates volume concentration.

Drop Classes used in the Calculations

Critical radius vs. Dry radius



Critical supersaturation



Color code allows history of individual drop classes to be readily followed.

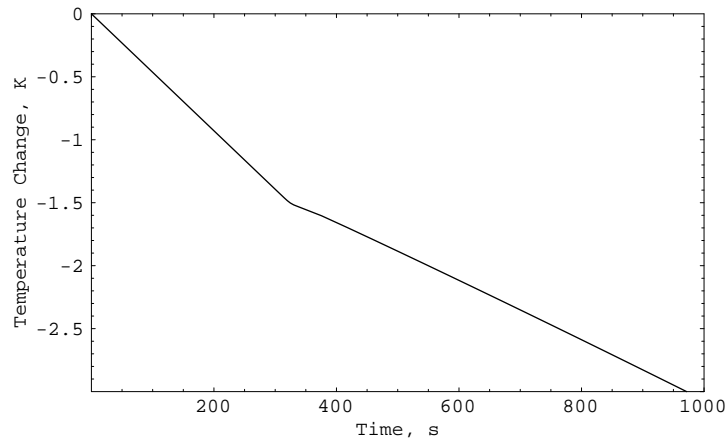
Particles are treated as $(\text{NH}_4)_2\text{SO}_4$.

Largest four classes (sea salt) are omitted in most calculations.

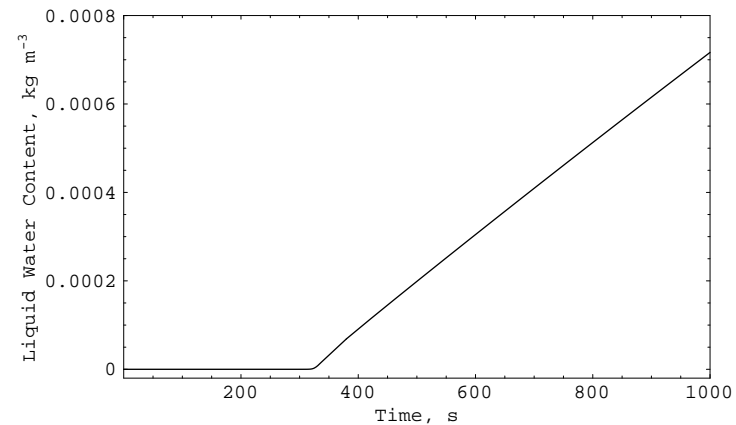
Example Results

Updraft velocity w taken as 0.5 m s^{-1} , typical of moderately strong updraft (stratocumulus).
Calculation starts at relative humidity 90%, with dry adiabatic lapse rate.
 $(\text{NH}_4)_2\text{SO}_4$ mass loading $0.275 \mu\text{g m}^{-3}$; mixing ratio $0.048 \text{ nmol/mol}(\text{air})$ (ppb).

Temperature Change

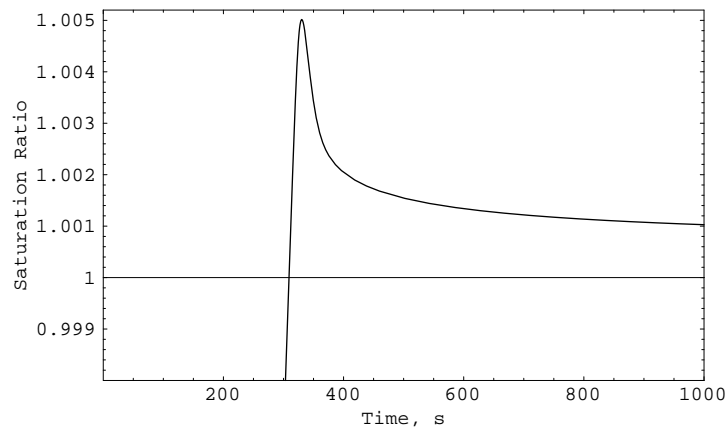


Liquid Water Content

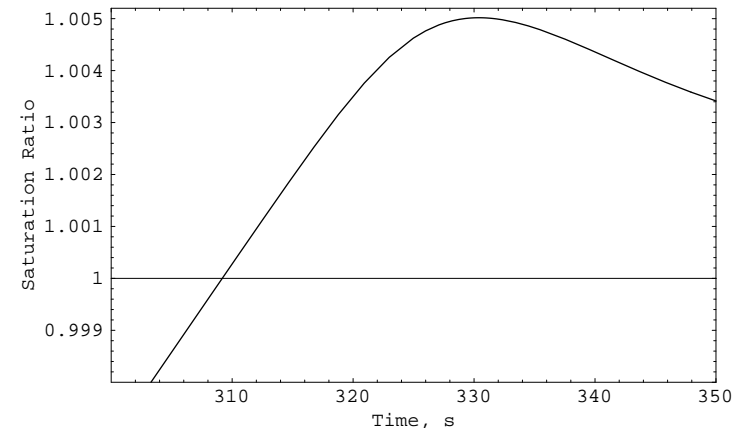


Break at $\sim 320 \text{ s}$ is due to latent heat release at onset of cloud formation.

Saturation Ratio

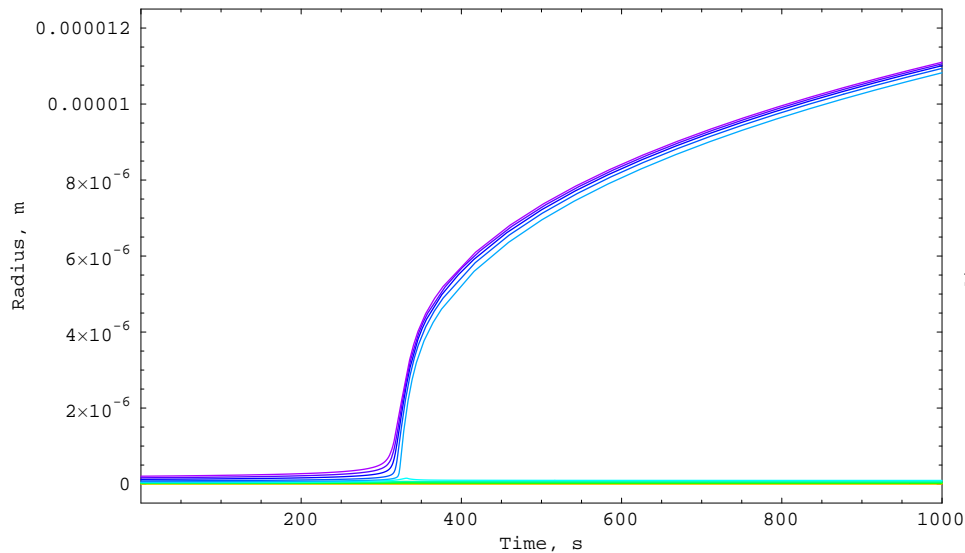


Zoom in



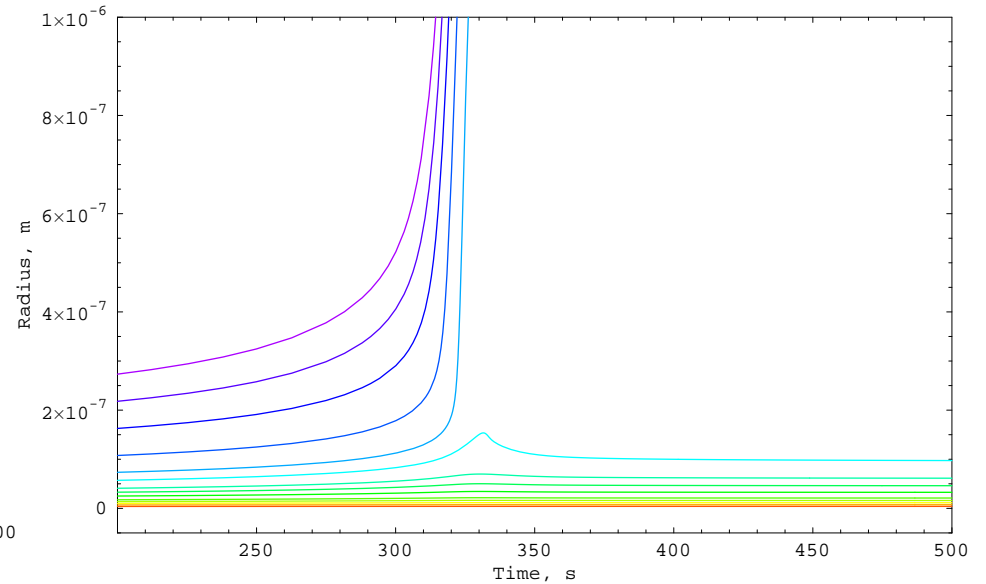
Note **sharp maximum in saturation ratio** followed by decrease as water vapor condenses on newly activated cloud drops.

Drop Radii vs. time



Note abrupt change of drop radii upon activation.
Note compression of cloud drop spectrum.

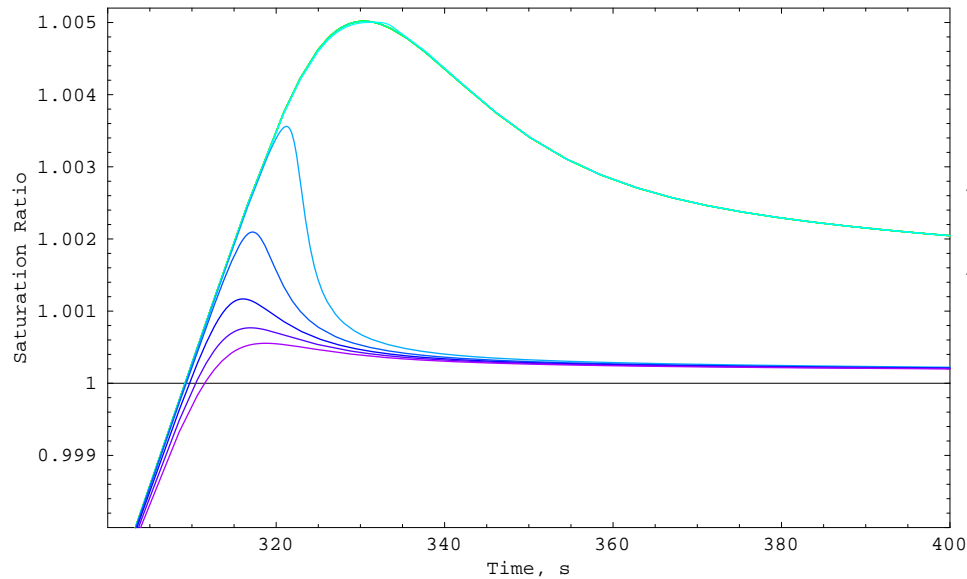
Zoom in on activation region



Note “knife-edge” separation of activated and unactivated particles.
Unactivated particles grow and shrink as saturation ratio increases and then decreases as water is taken up on activated droplets.

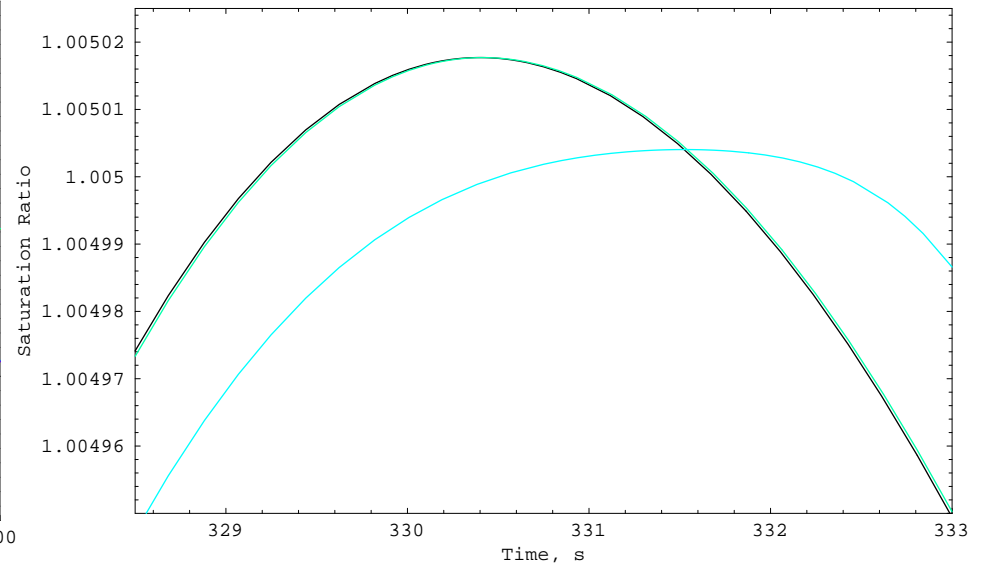
Saturation ratio

Equilibrium (Köhler) saturation ratio



Unactivated droplets exhibit saturation ratio equal to that of the environment, also plotted but hidden under the nest of curves at the top.

Zoom in on activation region

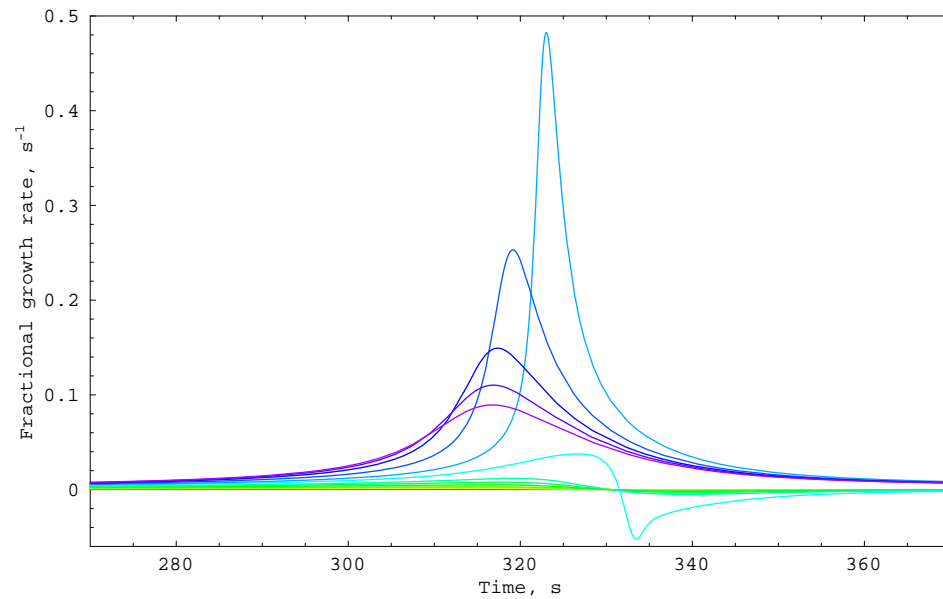


Colors denote last two classes of unactivated drops; black curve denotes environmental saturation ratio.

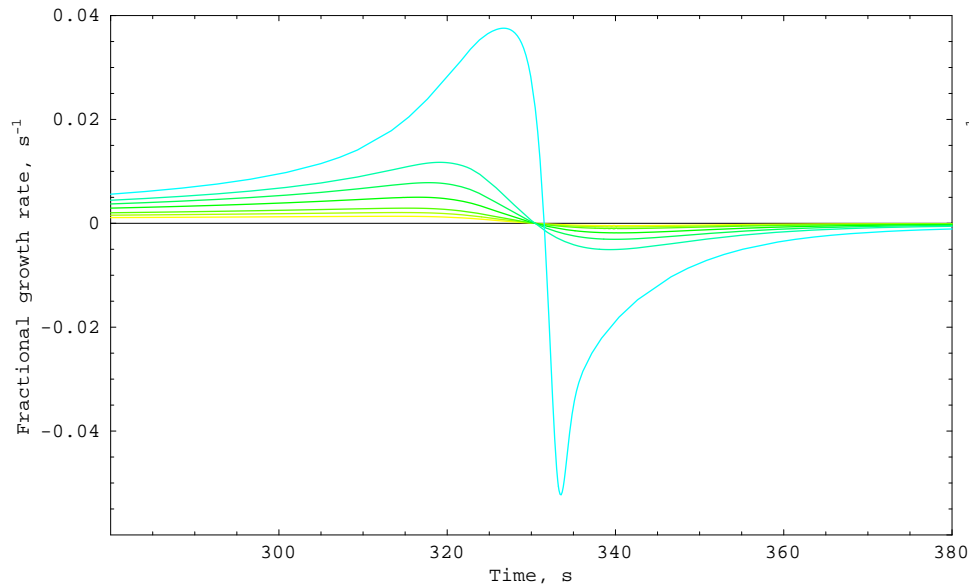
Note slight lag in equilibrium saturation ratio due to mass-transport kinetics.

Droplet Growth Kinetics

Fractional rate of change of radius
of particles during activation $\frac{1}{a} \frac{da}{dt}$

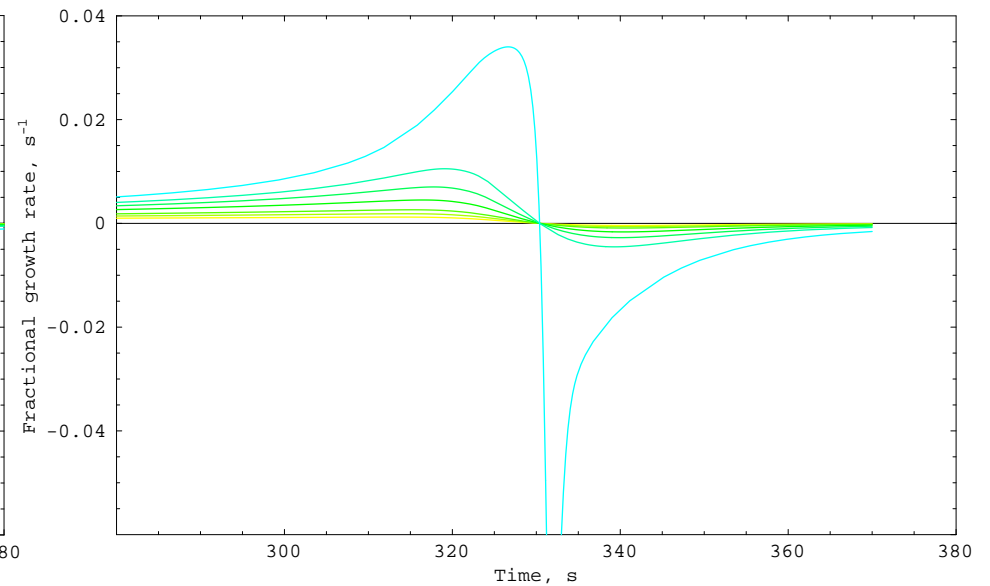


Growth and Shrink of Unactivated Drops



Fractional growth evaluated as $\frac{1}{a} \frac{da}{dt}$

Equilibrium Growth and Shrink Kinetics

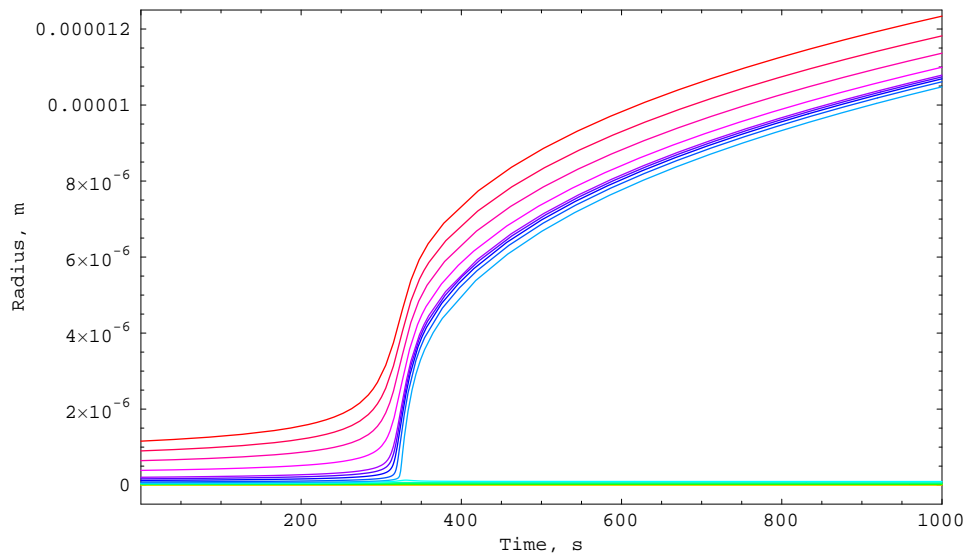


Evaluated as $\frac{1}{a_{eq}} \frac{da_{eq}}{dt} = \frac{1}{a_{eq}} \frac{da_{eq}}{dp_w} \frac{dp_w}{dt}$

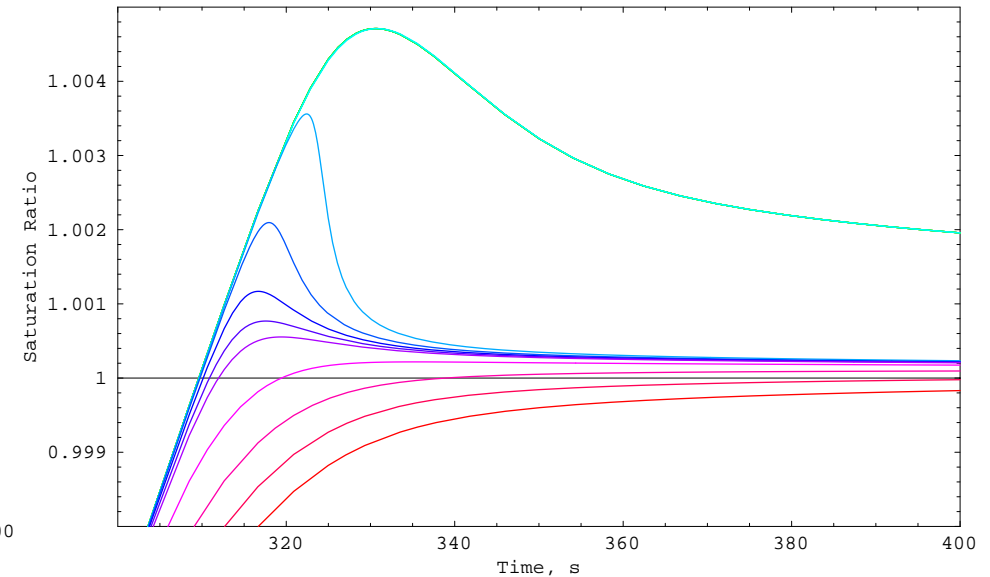
The near equality establishes that **mass transport kinetics are not limiting activation** of the drops under these conditions; contrast Chuang, Charlson & Seinfeld (1997).

Results with sea salt included

Drop Radii vs. time



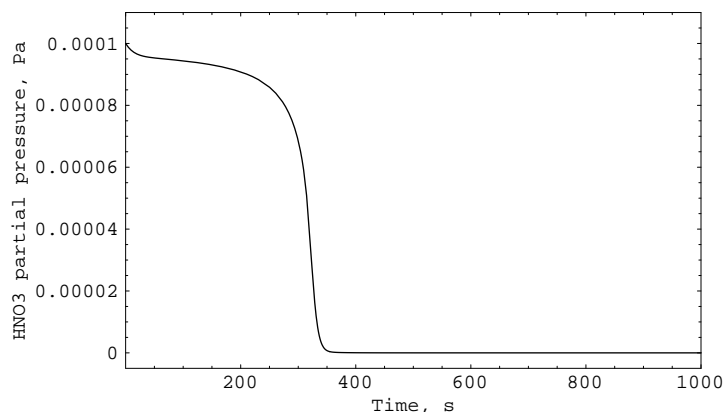
Equilibrium (Köhler) saturation ratio



Sea salt droplets get a “head start” and the rest of the cloud droplets never catch up. The three largest classes of droplets **never reach supersaturation** but are effectively cloud droplets anyway, as pointed out by Hänel (1987).

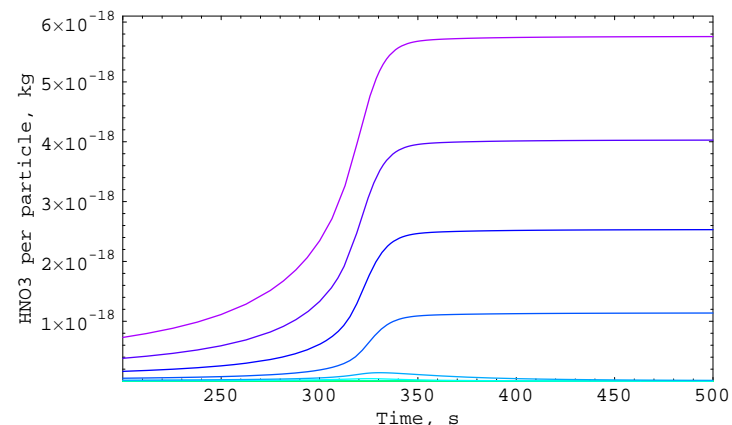
Results with 1 ppb HNO_3 included

HNO_3 partial pressure vs. time



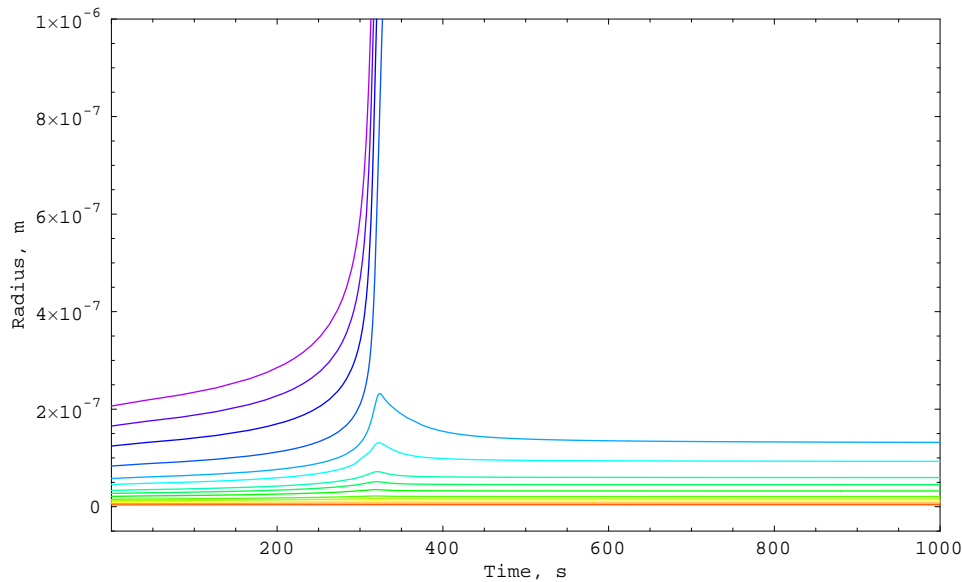
Note abrupt decrease as drops activate.

HNO_3 mass in activated drops vs. time

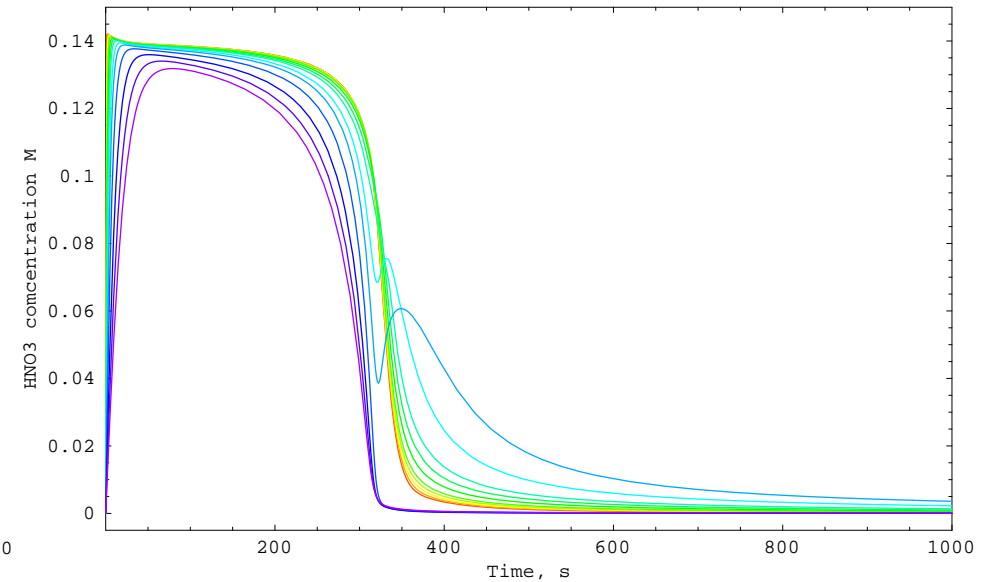


After activation mass is constant because low HNO_3 vapor pressure precludes exchange among drops.

Zoom on radius vs. time



HNO₃ aqueous concentration vs. time



HNO₃ aqueous concentration exerts a complex behavior that reflects mass transport of water vapor and HNO₃ and droplet growth (dilution).

As drops activate HNO₃ concentration rapidly decreases because of dilution.

HNO₃ concentration in last two unactivated classes increases as drop radii decrease as water transfers to newly activated drops.

The nonuniform HNO₃ concentrations would be expected to influence strongly pH-dependent reactions such as aqueous oxidation of SO₂ by O₃.

Summary of Results

| (NH ₄) ₂ SO ₄ mass loading | (NH ₄) ₂ SO ₄ mixing ratio | Updraft velocity | Maximum Super- saturation | Droplet Number Conc. | Fraction NSS mass scavenged |
|---|---|---------------------|---------------------------------|----------------------------|-----------------------------------|
| μg m ⁻³ | nmol/mol(air) (ppb) | m s ⁻¹ | % | cm ⁻³ | |
| 2.75 | 0.48 | 0.5 | 0.26 | 997 | 0.935 |
| 0.275 | 0.048 | 0.5 | 0.50 | 140 | 0.955 |
| 0.275 + seasalt | 0.048 + 0.64 | 0.5 | 0.47 | 140 | 0.955 |
| 27.5 | 4.8 | 0.5 | 0.11 | 3150 | 0.66 |
| 2.75 | 0.48 | 2.0 | 0.51 | 1298 | 0.955 |
| 2.75 + HNO ₃ | 0.48 + 1 | 0.5 | 0.22 | 997 | 0.935 |

Conclusions

A **highly flexible model** (“desktop cloud”) has been presented that describes the mass-transport kinetics of water vapor condensation and cloud droplet activation.

The input parameters to the model can readily be changed to study cloud droplet activation for any situation of interest.

This model readily displays drop-size dependent processes occurring during cloud formation.

For the cases studied the **mass transport of water vapor is sufficiently fast that Köhler equilibrium can be assumed for activating drops.**

Large drops may not activate but become effective cloud drops anyway.

The reversible uptake of even a highly soluble gas such as HNO_3 exerts a complex dependence on drop size and time.

This model can be used to develop parameters for large scale models or to test alternative formulations such as moment methods.

Acknowledgment

This work was supported by the Department of Energy through its Atmospheric Chemistry Program.

This presentation is available on the web at

<http://www.ecd.bnl.gov/steve/pubs.html>
